A Convergent Reaction-Diffusion Master Equation

S. A. Isaacson
*Department of Mathematics and Statistics, Boston University, MA, USA**

The reaction-diffusion master equation (RDME) is a lattice stochastic reaction-diffusion model that has been used to study spatially distributed cellular processes. The RDME has been shown to have the drawback of losing bimolecular reactions in the continuum limit that the lattice spacing approaches zero (in two or more dimensions). In this work we derive a new convergent RDME (CRDME) that eliminates this problem. The CRDME is obtained by finite volume discretization of a spatially-continuous stochastic reaction-diffusion model. We demonstrate the empirical numerical convergence of reaction time statistics associated with the CRDME. Although the reaction time statistics of the RDME diverge as the lattice spacing approaches zero, we show they approach those of the CRDME for sufficiently large lattice spacings or slow bimolecular reaction rates. As such, the RDME may be interpreted as an approximation to the CRDME in several asymptotic limits.

I. INTRODUCTION

Computational models of biochemical systems within individual cells have become a common tool used in studying cellular processes and behavior [22, 31, 34, 42]. The spatially distributed nature of chemical pathways inside cells may, in certain cases, be more accurately modeled by including the explicit spatial movement of molecules. Examples of such processes include whether signals can propagate from the plasma membrane to nucleus [33], how cell shape can modify information flow in signaling networks [34], how the variable density of chromatin influences the search time of proteins for DNA binding sites [26], or how different regions of cytosolic space may separate to different chemical states [10].

One important consideration in developing these models is that at the scale of a single cell many biochemical processes are stochastic [2, 4, 35]. Stochastic reaction-diffusion models have been used to account for the stochasticity inherent in the chemical reaction process and the diffusion of proteins and mRNAs. These models approximate *individual molecules* as points diffusing within cells. They are more macroscopic descriptions than quantum mechanical or molecular dynamics models, which can resolve detailed interactions between a few molecules on timescales of milliseconds [36]. They are more microscopic descriptions than *deterministic* three-dimensional reaction-diffusion PDEs for the average concentration of each species of molecule.

Three stochastic reaction-diffusion models that have been used to study cellular processes are: the Doi model [6, 7, 39], the Smoluchowski diffusion limited reaction model (SDLR) [29, 37], and the reaction-diffusion master equation (RDME) [13, 16, 17, 24, 27, 40]. In the Doi model [6, 7] positions of molecules are represented as points undergoing Brownian motion. Bimolecular reactions between two molecules occur with a fixed probability per unit time when two reactants are separated by *less* than some specified "reaction radius". The SDLR model differs by representing bimolecular reactions in one of two ways; either occurring instantaneously, or with fixed probability per unit time, when two reactants' separation is *exactly* the reaction-radius [29, 37]. In each of the models unimolecular reactions represent internal processes. They are assumed to occur with exponentially distributed times based on a specified reaction-rate constant.

The RDME can be interpreted as an extension of the non-spatial chemical master equation (CME) [16, 17, 32, 40] model for stochastic chemical kinetics. In the RDME space is partitioned by a mesh into a collection of voxels. The diffusion of molecules is modeled as a continuous time random walk on the mesh, with bimolecular reactions occurring with a fixed probability per unit time for molecules within the same voxel. Within each voxel molecules are assumed well-mixed (*i.e.* uniformly distributed), and molecules of the same species are indistinguishable. Mathematically, the RDME is the forward Kolmogorov equation for a continuous-time jump Markov process.

In each of the three models the state of the chemical system is given by stochastic processes for the number of molecules of each chemical species and the corresponding positions of each molecule. There are two different mathematical formulations of each model; either coupled systems of equations for the probability densities of having a given state at a specified time, or equations for the evolution of the stochastic processes themselves. The former description leads to, possibly infinite, coupled systems of partial integral differential equations (PIDEs) for the Doi/SDLR models, and, possibly infinite, coupled systems of ordinary differential equations (ODEs) for the RDME. The high dimensionality of these equations for typical biological systems prevents the use of standard numerical methods for PDEs/ODEs in low-dimensions. Instead, the probability density solutions to these equations are approximated by simulating the underlying stochastic processes by Monte Carlo methods [1, 5, 8, 12, 18, 38].

While the RDME can be used as an independent model, in applications it is often interpreted as a formal approximation of the Doi or SDLR models [14]. In

* isaacson@math.bu.edu

practice, using the RDME to approximate either of the Doi or SDLR models can be problematic as it has been shown that in the continuum limit where the mesh spacing in the RDME is taken to zero bimolecular reactions are lost [21, 24] (in two or more dimensions). That is, the time at which two molecules will react becomes infinite as the mesh spacing is taken to zero. In general the RDME can only provide a reasonable approximation to the Doi or SDLR models for mesh spacings that are neither too large or too small [25]. This error in this approximation can not be made arbitrarily small [25].

In this work we discretize the Doi model so as to obtain a forward Kolmogorov equation describing a continuous-time jump Markov process similar to the RDME. We seek a discretization of this form so that we may use Monte Carlo methods to simulate the underlying stochastic process for systems of many reacting molecules. Our convergent RDME (CRDME) approximates the Doi model, but retains bimolecular reactions as the mesh spacing approaches zero. In particular, for T the random variable for the time at which two molecules react, we show in two-dimensions by numerical simulation that both the survival time distribution, $\Pr[T > t]$, and the mean reaction time converge to finite values as the mesh spacing approaches zero in the CRDME (in contrast to the RDME).

The new CRDME retains many of the benefits of the original RDME model, and allows the re-use of the many extensions of the RDME that have been developed. Examples of these extensions include Cartesian-grid methods for complex geometries [27]; the incorporation of drift due to potentials [26, 43]; advective velocity fields [20]; non-Cartesian meshes [11]; GPU optimized simulation methods [41]; adaptive mesh refinement techniques (AMR) to improve the approximation of molecular diffusion [3]; and multiscale couplings to more macroscopic models [15]. In addition to retaining bimolecular reactions as the mesh spacing approaches zero, we show that the CRDME is approximable by the RDME for appropriate mesh spacings and parameter choices.

II. GENERAL DOI AND RDME MODELS

We first illustrate how the bimolecular reaction A + B $\to$ C would be described by the Doi model and the standard RDME in $\mathbb{R}^d$. In the Doi model, bimolecular reactions are characterized by two parameters; the separation at which molecules may begin to react, $r_{\rm b}$, and the probability per unit time the molecules react when within this separation, λ. When a molecule of species A and a molecule of species B react we assume the C molecule they produce is placed midway between them. Note the important point that in each of the models molecules are modeled as points.

We now formulate the Doi model as an infinite coupled system of partial integral differential equations (PIDEs). Let $\boldsymbol{q}_l^a \in \mathbb{R}^d$ denote the position of the lth molecule of species A when the total number of molecules of species A is a. The state vector of the species A molecules is then given by $\boldsymbol{q}^a = (\boldsymbol{q}_1^a, \ldots, \boldsymbol{q}_a^a) \in \mathbb{R}^{da}$. Define $\boldsymbol{q}^b$ and $\boldsymbol{q}^c$ similarly. We denote by $f^{(a,b,c)}(\boldsymbol{q}^a, \boldsymbol{q}^b, \boldsymbol{q}^c, t)$ the probability density for there to be a molecules of species A, b molecules of species B, and c molecules of species C at time t located at the positions $\boldsymbol{q}^a$, $\boldsymbol{q}^b$, and $\boldsymbol{q}^c$. Molecules of the same species are assumed indistinguishable. The evolution of $f^{(a,b,c)}$ is given by

$$\frac{\partial f^{(a,b,c)}}{\partial t}\left(\boldsymbol{q}^a, \boldsymbol{q}^b, \boldsymbol{q}^c, t\right) = (L+R)\, f^{(a,b,c)}\left(\boldsymbol{q}^a, \boldsymbol{q}^b, \boldsymbol{q}^c, t\right). \tag{1}$$

Note, with the subsequent definitions of the operators L and R this will give a coupled system of PIDEs over all possible values of (a, b, c). More general systems that allow unbounded production of certain species would result in an infinite number of coupled PIDEs. The diffusion operator, L, is defined by

$$Lf^{(a,b,c)} = \left[D^{\rm A}\sum_{l=1}^{a}\Delta_l^a + D^{\rm B}\sum_{m=1}^{b}\Delta_m^b + D^{\rm C}\sum_{n=1}^{c}\Delta_n^c\right] f^{(a,b,c)}, \tag{2}$$

where Δ_l^a denotes the Laplacian in the coordinate $\boldsymbol{q}_l^a$ and $D^{\rm A}$ the diffusion constant of species A. $D^{\rm B}$, $D^{\rm C}$, Δ_m^b, and Δ_n^c are defined similarly.

To define the reaction operator, R, we introduce notations for removing or adding a specific molecule to the state $\boldsymbol{q}^a$. Let

$$\begin{aligned}\boldsymbol{q}^a \setminus \boldsymbol{q}_l^a &= \left(\boldsymbol{q}_1^a, \ldots, \boldsymbol{q}_{l-1}^a, \boldsymbol{q}_{l+1}^a, \ldots, \boldsymbol{q}_a^a\right),\\ \boldsymbol{q}^a \cup \boldsymbol{q} &= \left(\boldsymbol{q}_1^a, \ldots, \boldsymbol{q}_a^a, \boldsymbol{q}\right).\end{aligned}$$

$\boldsymbol{q}^a \setminus \boldsymbol{q}$ will denote $\boldsymbol{q}^a$ with any one component with the value $\boldsymbol{q}$ removed. Denote by $\mathbb{1}_{[0,r_{\rm b}]}(r)$ the indicator function of the interval $[0, r_{\rm b}]$, and let $B_l^c = \{\boldsymbol{q} \in \mathbb{R}^d \,|\, |\boldsymbol{q} - \boldsymbol{q}_l^c| \le r_{\rm b}/2\}$ label the set of points a reactant could be at to produce a molecule of species C at $\boldsymbol{q}_l^c$. The Doi reaction operator, R, is then

$$\begin{aligned}&\left(Rf^{(a,b,c)}\right)\left(\boldsymbol{q}^a, \boldsymbol{q}^b, \boldsymbol{q}^c, t\right) = \lambda\Bigg[\sum_{l=1}^{c}\\ &\int_{B_l^C} f^{(a+1,b+1,c-1)}\left(\boldsymbol{q}^a \cup \boldsymbol{q}, \boldsymbol{q}^b \cup \left(2\boldsymbol{q}_l^c - \boldsymbol{q}\right), \boldsymbol{q}^c \setminus \boldsymbol{q}_l^c, t\right) d\boldsymbol{q}\\ &- \sum_{l=1}^{a}\sum_{l'=1}^{b}\mathbb{1}_{[0,r_{\rm b}]}\left(\left|\boldsymbol{q}_l^a - \boldsymbol{q}_{l'}^b\right|\right) f^{(a,b,c)}(\boldsymbol{q}^a, \boldsymbol{q}^b, \boldsymbol{q}^c, t)\Bigg].\end{aligned} \tag{3}$$

We now describe the RDME, in a form we derived in [23] that has the advantage of representing a chemical system's state in a similar manner to the Doi model. Using this representation allows for easier comparison of the RDME and Doi models. Partition $\mathbb{R}^d$ into a Cartesian lattice of voxels with width h and hypervolume h^d. When in the *same* voxel, an A and B molecule may react with probability per unit time k/h^d. Here k represents

the macroscopic bimolecular reaction-rate constant of the reaction $\mathrm{A}+\mathrm{B}\to\mathrm{C}$, with units of hypervolume per unit time. Let $\boldsymbol{j}_l^a \in \mathbb{Z}^d$ denote the multi-index of the voxel centered at $h\boldsymbol{j}_l^a$ that contains the lth molecule of species A when there are a molecules of species A. The position of the molecule is assumed to be uniformly distributed (*i.e.* well-mixed) within this voxel. Let $\boldsymbol{j}^a = (\boldsymbol{j}_1^a, \ldots, \boldsymbol{j}_a^a)$ denote the state vector for the voxels containing the a molecules of species A. Define $\boldsymbol{j}^b$ and $\boldsymbol{j}^c$ similarly, and let $F_h^{(a,b,c)}(\boldsymbol{j}^a, \boldsymbol{j}^b, \boldsymbol{j}^c, t)$ denote the probability that there are (a,b,c) molecules of species A, B, and C at time t in the voxels given by $\boldsymbol{j}^a$, $\boldsymbol{j}^b$, and $\boldsymbol{j}^c$. The RDME is then the coupled system of ODEs over all possible values for a, b, c, $\boldsymbol{j}^a$, $\boldsymbol{j}^b$, and $\boldsymbol{j}^c$,

$$\frac{dF_h^{(a,b,c)}}{dt}\left(\boldsymbol{j}^a, \boldsymbol{j}^b, \boldsymbol{j}^c, t\right) = (L_h + R_h)\, F_h^{(a,b,c)}\left(\boldsymbol{j}^a, \boldsymbol{j}^b, \boldsymbol{j}^c, t\right), \tag{4}$$

where L_h is a discretized approximation to L given by

$$L_h F_h^{(a,b,c)}\left(\boldsymbol{j}^a, \boldsymbol{j}^b, \boldsymbol{j}^c, t\right) = \left(D^{\mathrm{A}}\Delta_h^a + D^{\mathrm{B}}\Delta_h^b + D^{\mathrm{C}}\Delta_h^c\right) F_h^{(a,b,c)}\left(\boldsymbol{j}^a, \boldsymbol{j}^b, \boldsymbol{j}^c, t\right).$$

Here Δ_h^a denotes the standard da-dimensional discrete Laplacian acting in the $\boldsymbol{j}^a$ coordinate. We define the "standard" d-dimensional discrete Laplacian acting on a mesh function, $f(\boldsymbol{j})$ on $\mathbb{Z}^d$, by

$$\Delta_h f(\boldsymbol{j}) = \frac{1}{h^2}\sum_{k=1}^{d}\left[f(\boldsymbol{j}+\boldsymbol{e}_k) + f(\boldsymbol{j}-\boldsymbol{e}_k) - 2f(\boldsymbol{j})\right], \tag{5}$$

where $\boldsymbol{e}_k$ denotes a unit vector along the kth coordinate axis of $\mathbb{R}^d$.

The reaction operator, R_h, is given by

$$\left(R_h F_h^{(a,b,c)}\right)\left(\boldsymbol{j}^a, \boldsymbol{j}^b, \boldsymbol{j}^c, t\right) = \frac{k}{h^d}\left[\sum_{l=1}^{c} F_h^{(a+1,b+1,c-1)}\left(\boldsymbol{j}^a \cup \boldsymbol{j}_l^c, \boldsymbol{j}^b \cup \boldsymbol{j}_l^c, \boldsymbol{j}^c \setminus \boldsymbol{j}_l^c, t\right) - \sum_{l=1}^{a}\sum_{m=1}^{b}\delta_h\left(\boldsymbol{j}_l^a - \boldsymbol{j}_m^b\right) F_h^{(a,b,c)}\left(\boldsymbol{j}^a, \boldsymbol{j}^b, \boldsymbol{j}^c, t\right)\right], \tag{6}$$

where $\delta_h(\boldsymbol{j}_l^a - \boldsymbol{j}_m^b)$ denotes the Kronecker delta function equal to one when $\boldsymbol{j}_l^a = \boldsymbol{j}_m^b$ and zero otherwise. Note that these equations are a formal discrete approximation to the Doi model, where two molecules may now react when in the same voxel with rate k/h^d.

We have shown that the RDME (4) may be interpreted as a *formal* approximation to both Doi-like and Smoluchowski models [23–25]. As we proved in [24] and studied numerically in [25], the RDME loses bimolecular reactions as $h \to 0$. This was shown rigorously for $d = 3$, where the divergence was shown to be like h^{-1}. A simple modification of our argument shows bimolecular reactions are lost for all $d > 1$, with a divergence like $\ln(h)$ for $d = 2$, and like h^{-d+2} for $d > 2$. More recently asymptotic expansions were used in [21] to show the mean reaction time becomes infinite with the preceding rates as $h \to 0$ (for $d = 2$ or $d = 3$). This loss of reaction occurs because molecules are modeled by points, and as $h \to 0$ each voxel of the mesh shrinks to a point. Since two molecules must be in the same voxel to react, and in two or more dimensions two points can not find each other by diffusion, bimolecular reactions will never occur.

It should be noted that while the RDME loses bimolecular reactions in the limit that $h \to 0$, we have shown that for *fixed* values of h it gives an asymptotic approximation in the binding radius, r_{b}, to the SDLR model [24, 25]. How accurate this approximation can be made is dependent on domain geometry and the parameters of the underlying chemical system [25]. In particular, h must be chosen sufficiently large that reactions within a voxel can be approximated by a well-mixed reaction with rate k/h^d, while chosen sufficiently small that the diffusion of the molecules is well-approximated by a continuous time random walk on the mesh [10, 24].

In the next section we develop a new convergent RDME (CRDME) to overcome these limitations of the standard RDME (4).

III. A CONVERGENT RDME (CRDME)

To construct a convergent RDME (CRDME) we use a finite volume discretization of the Doi PIDEs (1). For brevity we illustrate our approach on a simplified version of (1) when there is only one molecule of A and one molecule of B in the system which may undergo the annihilation reaction $\mathrm{A}+\mathrm{B}\to\varnothing$. The approach we describe can be extended to general multi-particle systems as bimolecular reactions in the Doi model only involve multiple two-particle interactions of the same form, see (1).

For now we work in d-dimensional free-space, $\mathbb{R}^d$ (for most biological models $d = 2$ or $d = 3$). Denote by $\boldsymbol{x} \in \mathbb{R}^d$ the position of the molecule of species A and by $\boldsymbol{y} \in \mathbb{R}^d$ the position of the molecule of species B. In the Doi model these molecules diffuse independently, and may react with probability per unit time λ when within a separation r_{b}. (r_{b} is usually called the reaction-radius.) We let $\mathcal{R} = \{(\boldsymbol{x}, \boldsymbol{y}) \mid |\boldsymbol{x} - \boldsymbol{y}| < r_{\mathrm{b}}\}$, and denote the indicator function of this set by $\mathbb{1}_{\mathcal{R}}(|\boldsymbol{x} - \boldsymbol{y}|)$. The diffusion constants of the two molecules will be given by D^{A} and D^{B} respectively.

Finally, we denote by $p(\boldsymbol{x}, \boldsymbol{y}, t)$ the probability density the two molecules have not reacted and are at the positions $\boldsymbol{x}$ and $\boldsymbol{y}$ at time t. Then (1) reduces to

$$\frac{\partial p}{\partial t}(\boldsymbol{x}, \boldsymbol{y}, t) = (D^{\mathrm{A}}\Delta_{\boldsymbol{x}} + D^{\mathrm{B}}\Delta_{\boldsymbol{y}})p(\boldsymbol{x}, \boldsymbol{y}, t) - \lambda\mathbb{1}_{\mathcal{R}}(|\boldsymbol{x} - \boldsymbol{y}|)p(\boldsymbol{x}, \boldsymbol{y}, t). \tag{7}$$

(Here we have dropped the equation for the state $a = 0$, $b = 0$.)

We now show how to construct a new type of RDME by discretization of this equation. Note, while (7) can be solved analytically by switching to the separation coordinate, $\boldsymbol{x}-\boldsymbol{y}$, such approaches will not work for more general chemical systems, such as (1). As such, we illustrate our CRDME ideas on (7), though ultimately they are intended for use in modeling more complex chemical systems with many chemical species, reactions, and complex geometries. For $\boldsymbol{i}\in\mathbb{Z}^d$ and $\boldsymbol{j}\in\mathbb{Z}^d$ we partition $\mathbb{R}^{2d}$ into a Cartesian grid of hypercubes, labeled by $V_{\boldsymbol{ij}}$. We assume $V_{\boldsymbol{ij}}$ has coordinate-axis aligned edges with length h and center $(\boldsymbol{x_i},\boldsymbol{y_j})=(\boldsymbol{i}h,\boldsymbol{j}h)$. We denote the hypervolume of a set, S, by $|S|$. For example, the hypervolume of the hypercube $V_{\boldsymbol{ij}}$ is $|V_{\boldsymbol{ij}}|=h^{2d}$.

We make the *approximation* that the probability $(\boldsymbol{x},\boldsymbol{y})\in V_{\boldsymbol{ij}}$ at time t is given by $P_{\boldsymbol{i},\boldsymbol{j}}(t)=p(\boldsymbol{x_i},\boldsymbol{y_j},t)\times|V_{\boldsymbol{ij}}|$. Note that $P_{\boldsymbol{i},\boldsymbol{j}}(t)$ equivalently gives the probability that the particle of species A is in the d-dimensional hypercube of length h centered about $\boldsymbol{i}h$, while the particle of species B is in the d-dimensional hypercube of length h about the point $\boldsymbol{j}h$. Using this assumption we construct a finite volume discretization of (7) by integrating both sides of (7) over the hypercube $V_{\boldsymbol{ij}}$. As we did in [27], we make the standard finite volume approximations for the integrals involving $\Delta_{\boldsymbol{x}}p$ and $\Delta_{\boldsymbol{y}}p$ to obtain discrete Laplacians given by (5) in the $\boldsymbol{x}$ and $\boldsymbol{y}$ coordinates. The reaction term is approximated by

$$\begin{aligned}\lambda\int_{V_{\boldsymbol{ij}}}\mathbb{1}_{\mathcal{R}}(|\boldsymbol{x}-\boldsymbol{y}|)p(\boldsymbol{x},\boldsymbol{y},t)\,d\boldsymbol{x}\,d\boldsymbol{y}&\\ \approx\frac{\lambda}{|V_{\boldsymbol{ij}}|}P_{\boldsymbol{i},\boldsymbol{j}}(t)\int_{V_{\boldsymbol{ij}}}\mathbb{1}_{\mathcal{R}}(|\boldsymbol{x}-\boldsymbol{y}|)\,d\boldsymbol{x}\,d\boldsymbol{y}&\\ =\frac{\lambda\,|\mathcal{R}\cap V_{\boldsymbol{ij}}|}{|V_{\boldsymbol{ij}}|}P_{\boldsymbol{i},\boldsymbol{j}}(t).&\end{aligned}$$

Define the volume fraction $\phi_{\boldsymbol{ij}}=|\mathcal{R}\cap V_{\boldsymbol{ij}}|/|V_{\boldsymbol{ij}}|$. Our discretization then represents a new RDME for the two-particle system, given by the coupled system of ODEs over all values of $(\boldsymbol{i},\boldsymbol{j})\in\mathbb{Z}^{2d}$,

$$\frac{dP_{\boldsymbol{i},\boldsymbol{j}}}{dt}(t)=L_hP_{\boldsymbol{i},\boldsymbol{j}}(t)-\lambda\phi_{\boldsymbol{ij}}P_{\boldsymbol{i},\boldsymbol{j}}(t). \tag{8}$$

Here $L_h=(D^{\mathrm{A}}L_h^{\mathrm{A}}+D^{\mathrm{B}}L_h^{\mathrm{B}})$, with L_h^{A} and L_h^{B} denoting standard d-dimensional discrete Laplacians (5) (in the $\boldsymbol{i}$ and $\boldsymbol{j}$ coordinates respectively). By choosing an appropriate discretization we have obtained an equation that has the form of the forward Kolomogorov equation for a continuous-time jump Markov process. We may therefore interpret the coefficients in (8) as transition rates, also called propensities, between states $(\boldsymbol{i},\boldsymbol{j})$ of the stochastic process. We subsequently refer to this equation as the CRDME. In the CRDME diffusion is handled in exactly the same manner as for the RDME. In contrast, the reaction mechanism in (8) now allows molecules in distinct voxels, $\boldsymbol{i}$ and $\boldsymbol{j}$, to react with a potentially non-zero probability per unit time, $\lambda\phi_{\boldsymbol{ij}}$.

As discussed earlier, the RDME is only physically valid when h is chosen sufficiently large that the timescale for two molecules to become uniformly distributed within a voxel by diffusion is much faster than that for a well-mixed bimolecular reaction to occur between them. By allowing molecules to react when in nearby voxels, our CRDME provides a correction when h is sufficiently small that this condition is violated. For $r_{\mathrm{b}}>h$ molecules may potentially react when separated by multiple voxels, with the number of voxels apart two molecules can be and still react increasing as $h\to 0$.

IV. EMPIRICAL CONVERGENCE OF THE CRDME

We now demonstrate that in two-dimensions ($d=2$) the survival time distribution and the mean reaction time for the CRDME (8) converge to finite values as $h\to 0$. We show that in the corresponding RDME model the survival time and mean reaction time diverge to ∞ as $h\to 0$. In contrast, in the opposite limit that $r_{\mathrm{b}}/h\to 0$ we demonstrate that the mean reaction time in the RDME approaches that of the CRDME. As (7) is a PDE in four-dimensions, we do not directly solve the corresponding system of ODEs given by the CRDME (8). Instead, we simulate the corresponding stochastic jump process for the molecule's motion and reaction by the well-known exact stochastic simulation algorithm (SSA) (also known as the Gillespie method [18] or kinetic Monte Carlo [5]).

We assume each molecule moves within a square with sides of length L, $\Omega=[0,L]\times[0,L]$, with zero Neumann boundary conditions. These boundary conditions are enforced by setting the transition rate for a molecule to hop from a given mesh voxel outside the domain to zero. For a specified number of mesh voxels, N, we discretize Ω into a Cartesian grid of squares with sides of length $h=L/N$. We assume $D^{\mathrm{A}}=D^{\mathrm{B}}=D$. Unless otherwise specified, all spatial units will be micrometers, with time in units of seconds. The SSA-based simulation algorithm can be summarized as:

1. Specify D, L, N, λ, and r_{b} as input.
2. Calculate $\phi_{\boldsymbol{0j}}$. (See the supplementary material.)
3. We assume the molecules are well-mixed at time $t=0$. That is, the initial position of each molecule is sampled from a uniform distribution among all voxels of the mesh.
4. Sample a time and direction of the next spatial hop by one of the molecules. (From (8) each molecule may hop to a neighbor in the x or y direction with probability per unit time D/h^2.)
5. Assuming the molecules are at $\boldsymbol{i}$ and $\boldsymbol{j}$, if $\phi_{\boldsymbol{ij}}\neq 0$ sample the next reaction time using the transition rate $\lambda\phi_{\boldsymbol{ij}}$.
6. Select the smaller of the hopping and reaction times, and execute that event. Update the current time to the time of the event.
7. If a reaction occurs the simulation ends. If a spatial hop occurs, return to 4.

For all simulations we chose $L=.2\,\mu$m. With this

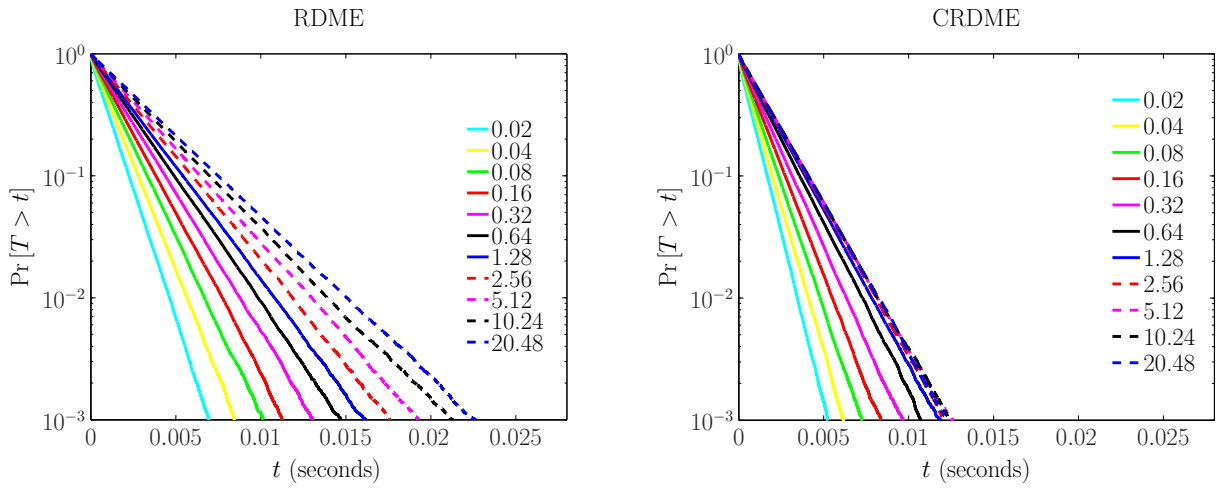

FIG. 1: Survival time distributions vs. t for the CRDME and RDME when $\lambda = 10^9\,\mathrm{s}^{-1}$. Each curve was estimated from 128000 simulations. The legends give the ratio, r_b/h, used for each curve (note that $r_\mathrm{b} = 1$nm was fixed and h successively halved). We see the convergence of the survival time distributions for the CRDME (up to sampling error), while the survival time distributions in the RDME diverge.

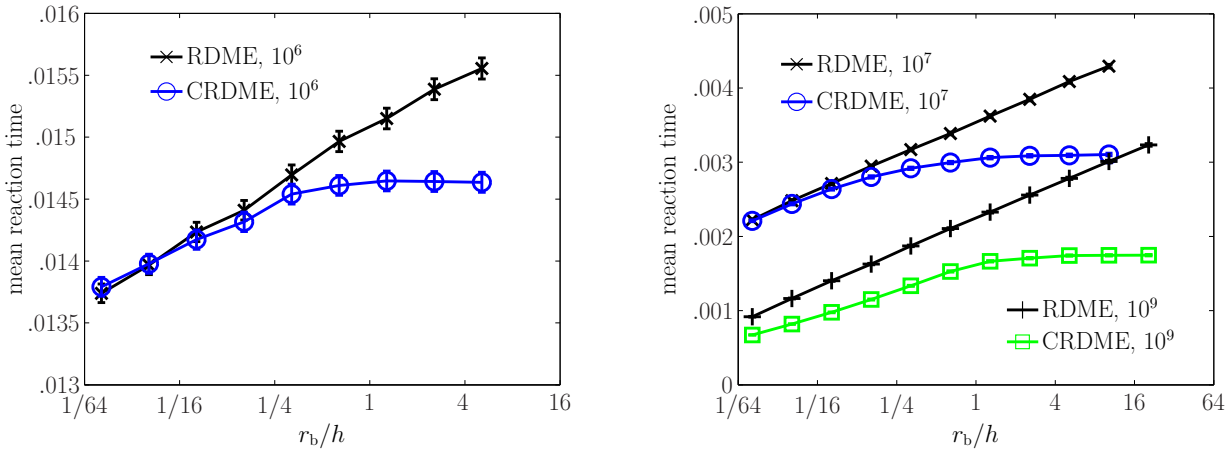

FIG. 2: Mean reaction times vs. r_b/h as h decreases by factors of two. Legends give the value of λ for each curve (with units of s^{-1}). Each mean reaction time was estimated from 128000 simulations. Note that 95% confidence intervals are drawn on each data point. (For some points they are smaller than the marker labeling the point.) Since we use a logarithmic x-axis, we see that for h sufficiently small the mean reaction time in the standard RDME diverges like $\ln(h)$, while in the CRDME the mean reaction time converges to a finite value.

choice the domain could be interpreted as small patch of membrane within a cell. A diffusion constant of $D = 10\,\mu\mathrm{m}^2\mathrm{s}^{-1}$ was used for each molecule. The reaction radius, r_b, was chosen to be 1 nm. While physical reaction radii are generally not measured experimentally, this choice falls between the measured width of the LexA DNA binding potential (≈ 5 angstroms [30]) and the 5 nm reaction radius used for interacting membrane proteins in [9].

We also simulated the stochastic process described by the corresponding RDME model. The bimolecular reaction rate was chosen to be $k = \lambda\pi r_\mathrm{b}^2$ to illustrate how the RDME approximates the CRDME as $r_\mathrm{b}/h \to 0$, but diverges as $r_\mathrm{b}/h \to \infty$. Our motivation for this choice is explained in the next section. The simulation algorithm was identical to that just described, except that step 2 was removed and step 5 modified so that two molecules could only react when within the same voxel (with prob-

ability per unit time $k = \lambda \pi r_b^2/h^2$).

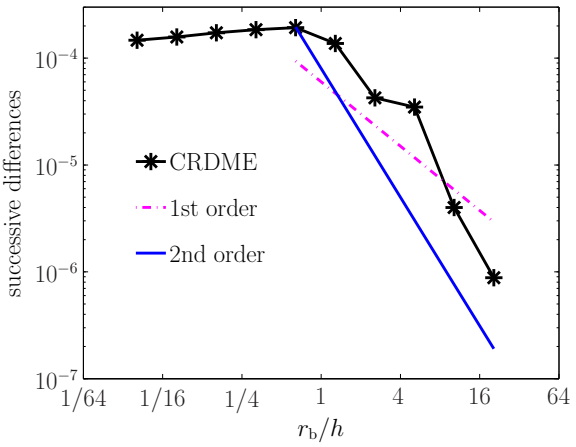

FIG. 3: Difference between successive points on the $\lambda = 10^9$ CRDME curve in Fig. 2 vs. r_b/h. The smaller of the two h values is used to label each point. The first and second order curves scale like h and h^2 respectively. Observe that the effective convergence rate to zero is closer to $O(h^2)$ than $O(h)$.

Let T denote the random variable for the time at which the two molecules react. The survival time distribution, $\Pr[T > t]$, is

$$\Pr[T > t] = \int_0^L \int_0^L p(\boldsymbol{x}, \boldsymbol{y}, t)\, d\boldsymbol{x}\, d\boldsymbol{y}.$$

Note that the reaction time distribution, $\Pr[T < t] = 1 - \Pr[T > t]$. We estimate $\Pr[T > t]$ from the numerically sampled reaction times using the MATLAB `ecdf` function. In Fig. 1 we show the convergence (to within sampling error) of the estimated survival time distributions for the CRDME (right figure) as $h \to 0$ (for $\lambda = 10^9 \mathrm{s}^{-1}$). In the left figure we show the divergence as $h \to 0$ of the estimated survival time distributions in the RDME. The continuing rightward shift of the distribution as the mesh width is decreased to twenty times finer than the reaction radius shows the divergence of the reaction time to infinity.

The mean reaction time, $\mathbb{E}[T]$, is given by

$$\mathbb{E}[T] = \int_0^\infty \Pr[T > t]\, dt.$$

We estimated $\mathbb{E}[T]$ from the numerically sampled reaction times by calculating the sample mean. Fig. 2 shows the estimated mean reaction times for the CRDME and RDME models as λ and r_b/h are varied (note the x-axis is logarithmic in r_b/h). We see that as $h \to 0$ the sampled mean reaction times in the CRDME converge to a fixed value. The rate of convergence in the CRDME for $\lambda = 10^9$ is illustrated in Fig. 3. There we plot the difference between successive estimated mean reaction times as h is halved. For small values of h this difference is seen to converge close to second order (as illustrated by the slope of the solid blue line).

In contrast, Fig. 2 shows that the sampled mean reaction time in the RDME diverges like $\ln(h)$ as discussed in [21, 24]. For all λ values the sampled mean reaction time in the RDME converges to that of the CRDME as $r_b/h \to 0$. As λ is decreased we see agreement between the RDME and CRDME for a larger range of r_b/h values.

Figs. 1, 2, and 3 demonstrate that, in contrast to the RDME, the reaction time statistics in the CRDME converge as $h \to 0$. That said, as $r_b/h \to 0$ we see that reaction time statistics of the RDME converge to those in the CRDME. Hence we may interpret the RDME as an approximation to the CRDME for $r_b/h \ll 1$. The *accuracy* of using this approximation to describe the reaction-diffusion process will then depend on the relative sizes of λ, D, and r_b as we discuss in the next section (and illustrated in Fig. 2).

V. RDME AS AN APPROXIMATION OF THE CRDME FOR $r_b/h \ll 1$

We now show that the RDME may be interpreted as an asymptotic approximation to the CRDME for $r_b/h \ll 1$, with the accuracy of this approximation depending on the size of D, r_b, and λ. In the standard RDME two molecules can only react when within the same d-dimensional voxel. (If k denotes a macroscopic bimolecular reaction rate, the probability per unit time the molecules react is usually chosen to be k/h^d, see (6).) In contrast, our new model allows two molecules to react when in neighboring voxels. Even for *large* values of h, the volume fraction $\phi_{\boldsymbol{ij}}$ will be non-zero when $\boldsymbol{i}$ and $\boldsymbol{j}$ are neighboring voxels. That said, for $\boldsymbol{j} \neq \boldsymbol{i}$ the volume fraction $\phi_{\boldsymbol{ij}}$ will approach zero quicker as $r_b/h \to 0$ than $\phi_{\boldsymbol{ii}}$. This relationship is shown in two-dimensions ($d = 2$) in Fig. 4. (We describe how the area fractions were calculated in the supplementary material.)

We therefore expect that, asymptotically, when $r_b/h \to 0$ the particles will effectively only react when $\boldsymbol{j} = \boldsymbol{i}$. In this case

$$\begin{aligned} |\mathcal{R} \cap V_{\boldsymbol{ii}}| &= \int_{\mathcal{R} \cap V_{\boldsymbol{ii}}} d\boldsymbol{y}\, d\boldsymbol{x} \\ &\approx \int_{[-h/2,h/2]^d} \int_{\{\boldsymbol{y} \,||\, \boldsymbol{x}-\boldsymbol{y}|<r_b\}} d\boldsymbol{y}\, d\boldsymbol{x} \\ &= |B_{r_b}|\, h^d, \end{aligned}$$

where $|B_{r_b}|$ denotes the volume of the d-dimensional sphere of radius r_b. The reaction rate when both particles are at the same position, $\boldsymbol{j} = \boldsymbol{i}$, is then

$$\lambda \phi_{\boldsymbol{ii}} = \frac{\lambda\, |\mathcal{R} \cap V_{\boldsymbol{ii}}|}{|V_{\boldsymbol{ii}}|} \approx \frac{\lambda\, |B_{r_b}|}{h^d}. \tag{9}$$

This corresponds to the choice of bimolecular reaction rate $k = \lambda\, |B_{r_b}|$ in the standard RDME. With this choice,

when $r_b/h \to 0$ the RDME may be interpreted as an asymptotic approximation of the CRDME. This approximation is illustrated in Fig. 2.

In three-dimensions, $d = 3$, the macroscopic bimolecular reaction rate $k = \lambda |B_{r_b}|$ also arises as the leading order asymptotic expansion as $r_b \to 0$, $\lambda \to 0$, or $D = D^A + D^B \to \infty$ of the diffusion limited bimolecular reaction rate for the Doi model (7), k_{Doi}. In [12] the latter was found to be

$$k_{\text{Doi}} = 4\pi D r_b \left(1 - \frac{1}{r_b}\sqrt{\frac{D}{\lambda}} \tanh\left(r_b\sqrt{\frac{\lambda}{D}}\right)\right).$$

(Note, the more well-known Smoluchowski diffusion limited reaction rate [29, 37], $k_{\text{Smol}} = 4\pi D r_b$, is recovered in the limit $\lambda \to \infty$.) As $r_b\sqrt{\lambda/D} \to 0$, $k_{\text{Doi}} \sim \lambda(4\pi r_b^3/3) = \lambda |B_{r_b}|$. We thus have that the CRDME recovers this well-mixed reaction rate as $r_b/h \to 0$. The smaller $r_b\sqrt{\lambda/D}$, the better the RDME should approximate the CRDME for fixed r_b/h.

When modeling three-dimensional biological systems, if $r_b\sqrt{\lambda/D}$ is sufficiently small h may simply be chosen to accurately model molecular diffusion by a continuous-time random walk. In this case, if $r_b/h \ll 1$ we may approximate the CRDME by the standard RDME. When these assumptions break down we need to decrease h and incorporate reactions between molecules in neighboring voxels with reactive transitions rates $\lambda\phi_{ij}$. The reaction and diffusion processes could potentially be decoupled by choosing separate meshes for each (as in [14]). That said, this process should be done so as to provide a convergent approximation of (7).

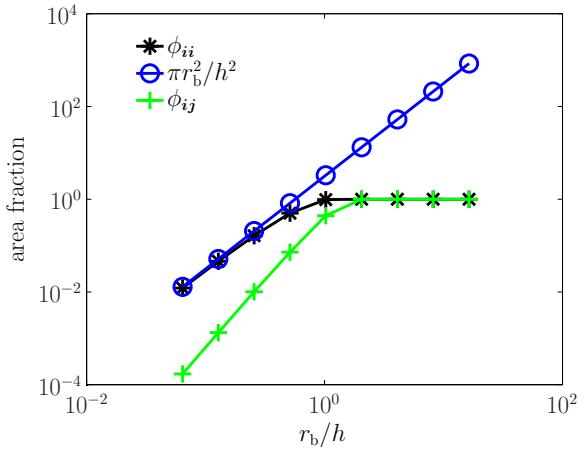

FIG. 4: Comparison of area fraction when both molecules are in the same square, ϕ_{ii}, with area fraction when the two molecules are in neighboring squares, ϕ_{ij}. We see that the area fraction decreases faster as $r_b/h \to 0$ when the two molecules are in different squares than when they are in the same square. Moreover, as $r_b/h \to 0$ the area fraction ϕ_{ii} approaches $\pi r_b^2/h^2$ as derived in (9).

VI. CONCLUSION

By discretizing the stochastic reaction-diffusion model of Doi [6, 7] we have derived a new convergent reaction-diffusion master equation. We illustrated our discretization procedure, and the convergence of the survival time distribution and mean reaction time in the CRDME, for two molecules that undergo the annihilation reaction $A + B \to \varnothing$. While this special case is simplified compared to realistic biological networks, it should be noted that the same reaction rates, $\lambda\phi_{ij}$, are derived when applying our discretization procedure to the more general multi-particle Doi model (1). Moreover, the same type of finite-volume approach we have taken to derive a CRDME approximating the Doi model could be applied to derive rates for approximating Smoluchowski models.

We do not show here that the CRDME provides a convergent discretization in d-dimensions. We hope to report on the convergence in three-dimensions for more realistic biological systems in the future.

Finally, it should be noted that while we have provided a method for deriving a convergent reaction-diffusion master equation as $h \to 0$, non-convergent reactive transition rates as derived in [12, 14, 21] may provide more accuracy in resolving specific statistics of underlying continuum stochastic reaction-diffusion models for *coarse* mesh widths ($h > r_b$). In particular, several of these works derive non-convergent reactive transition rates for use in the RDME that approximate statistics of Smoluchowski diffusion limited reaction models (as opposed to the Doi model we have studied).

ACKNOWLEDGMENTS

SAI is supported by NSF grant DMS-0920886.

SUPPLEMENTARY MATERIAL

VII. CALCULATION OF REACTION TRANSITION RATES

Denote by V_i the d-dimensional coordinate axis aligned hypercube with sides of length h centered at ih. With this definition we may then write $V_{ij} = V_i \times V_j$. We use $\hat{V}_i$ to denote this hypercube in the special case that $h = 1$. Finally, let $B_{r_b}(x)$ be the d-dimensional hypersphere of radius r_b about x. A convenient representation for ϕ_{ij} we subsequently use is

$$\phi_{ij} = \frac{1}{|V_{ij}|}\int_{V_i}\int_{V_j} \mathbb{1}_R(|x-y|)\,dy\,dx \tag{10}$$

$$= \frac{1}{|V_{ij}|}\int_{V_i} |B_{r_b}(x) \cap V_j|\,dx$$

$$= \int_{\hat{V}_0} \left|B_{r_b/h}(x) \cap \hat{V}_{j-i}\right|\,dx. \tag{11}$$

(Here $\mathbf{0}$ denotes the origin voxel.) Hence we may interpret $\phi_{\boldsymbol{ij}}$ as the integral over the center of a hypersphere of the volume of intersection between the hypersphere and a hypercube. The final equation (11) shows that $\phi_{\boldsymbol{ij}}$ depends on only two quantities; the separation vector $\boldsymbol{j}-\boldsymbol{i}$ and r_{b}/h. Also note that $\phi_{\boldsymbol{ij}}$ will be zero once the separation between all points in voxels $\boldsymbol{i}$ and $\boldsymbol{j}$ is more than r_{b}. As such, in practice it is only necessary to calculate $\phi_{\mathbf{0}\boldsymbol{j}}$ for a small number of voxels about the origin.

It is desirable to calculate $\phi_{\boldsymbol{ij}}$ to near machine precision to avoid the introduction of error from the use of incorrect reactive transition rates. While this may seem an easy task, simply calculating the hypervolume of intersection of $\mathcal{R}$ and $V_{\boldsymbol{ij}}$, it should be noted that these are four-dimensional (six-dimensional) sets when the molecules are in two-dimensions (three-dimensions). Evaluating $\phi_{\boldsymbol{ij}}$ by directly applying quadrature to (10) is complicated by the discontinuous integrand. We have found that several standard cubature [19, 28] and Monte Carlo methods [19] have difficultly evaluating such integrals in reasonable amounts of computing time to high numerical precision (absolute errors of near 10^{-12}). Since the integral (11) has a continuous integrand, which only requires the intersection of two-dimensional (three-dimensional) sets when the particles are each in two-dimensions (three-dimensions), we focus on evaluating $\phi_{\boldsymbol{ij}}$ through this representation.

To evaluate (11) both efficiently and accurately it is necessary to calculate the hypervolume of intersection given by the integrand, $v_{\boldsymbol{j}}(\boldsymbol{x}) = \left|B_{r_{\mathrm{b}}/h}(\boldsymbol{x}) \cap \hat{V}_{\boldsymbol{j}}\right|$. Our approach is based on writing this hypervolume as an integral and then converting to a boundary integral through the use of the divergence theorem. That is,

$$\begin{aligned} v_{\boldsymbol{j}}(\boldsymbol{x}) &= \frac{1}{d}\int_{B_{r_{\mathrm{b}}/h}(\boldsymbol{x})\cap\hat{V}_{\boldsymbol{j}}} \nabla\cdot\boldsymbol{y}\, d\boldsymbol{y}, \\ &= \frac{1}{d}\int_{\partial(B_{r_{\mathrm{b}}/h}(\boldsymbol{x})\cap\hat{V}_{\boldsymbol{j}})} \boldsymbol{y}\cdot\boldsymbol{\eta}(\boldsymbol{y})\, dS(\boldsymbol{y}), \\ &= \frac{1}{d}\int_{\partial B_{r_{\mathrm{b}}/h}(\boldsymbol{x})} (\boldsymbol{y}\cdot\boldsymbol{\eta}(\boldsymbol{y}))\, \mathbb{1}_{\hat{V}_{\boldsymbol{j}}}(\boldsymbol{y})\, dS(\boldsymbol{y}) \\ &\qquad + \frac{1}{d}\int_{\partial\hat{V}_{\boldsymbol{j}}} (\boldsymbol{y}\cdot\boldsymbol{\eta}(\boldsymbol{y}))\, \mathbb{1}_{B_{r_{\mathrm{b}}/h}(\boldsymbol{x})}(\boldsymbol{y})\, dS(\boldsymbol{y}). \quad (12) \end{aligned}$$

Here ∂M is used to denote the boundary of a manifold M, $\boldsymbol{\eta}(\boldsymbol{y})$ the outward normal to the boundary hypersurface at $\boldsymbol{y}$, and $dS(\boldsymbol{y})$ the hypersurface measure at $\boldsymbol{y}$.

For simplicity, in the remainder we assume $d = 2$. In this case we have developed a fast method, requiring only a few minutes on a modern laptop, that is able to evaluate (11) to near machine precision. $v_{\boldsymbol{j}}(\boldsymbol{x})$ is evaluated by calculating the intersection points of the circle $\partial B_{r_{\mathrm{b}}}(\boldsymbol{x})$ with the square $\hat{V}_{\boldsymbol{j}}$ numerically. Once these points are known the line integrals in (12) can be reduced to sums of integrals over sub-arcs where the indicator function is identically one or zero. These integrals can be evaluated analytically. Standard adaptive numerical quadrature methods, such as the `dblquad` routine in MATLAB, are then able to effectively integrate the area of intersection function $v_{\boldsymbol{j}}(\boldsymbol{x})$. This method was used to generate the area fractions in Fig. 4 and all SSA simulations.

[1] S. S. Andrews and D. Bray. Stochastic simulation of chemical reactions with spatial resolution and single molecule detail. *Physical Biology*, 1:137–151, 2004.

[2] A. Arkin and H. H. McAdams. Stochastic mechanisms in gene expression. *Proc. Natl. Acad. Sci. USA*, 94:814–819, February 1997.

[3] B. Bayati, P. Chatelain, and P. Koumoutsakos. Adaptive mesh refinement for stochastic reaction-diffusion processes. *J. Comp. Phys.*, 230(1):13–26, January 2011.

[4] W. J. Blake, M. Kaern, C. R. Cantor, and J. J. Collins. Noise in eukaryotic gene expression. *Nature*, 422:633–637, April 2003.

[5] A. B. Bortz, M. H. Kalos, and J. L. Lebowitz. A new algorithm for Monte Carlo simulation of Ising spin systems. *J. Comp. Phys.*, 17(1):10–18, 1975.

[6] M. Doi. Second quantization representation for classical many-particle system. *J. Phys. A: Math. Gen.*, 9(9):1465–1477, 1976.

[7] M. Doi. Stochastic theory of diffusion-controlled reaction. *J. Phys. A: Math. Gen.*, 9(9):1479–1495, 1976.

[8] A. Donev, V. V. Bulatov, T. Oppelstrup, G. H. Gilmer, B. Sadigh, and M. H. Kalos. A first-passage kinetic Monte Carlo algorithm for complex diffusion–reaction systems. *J. Comp. Phys.*, 229(9):3214–3236, January 2010.

[9] O. Dushek, P. A van der Merwe, and V. Shahrezaei. Ultrasensitivity in multisite phosphorylation of membrane-anchored proteins. *Biophys. J.*, 100(5):1189–1197, March 2011.

[10] J. Elf and M. Ehrenberg. Spontaneous separation of bistable biochemical systems into spatial domains of opposite phases. *IEE Sys. Biol.*, 1(2):230–236, December 2004.

[11] S Engblow, L Ferm, A Hellander, and P Lötstedt. Simulation of Stochastic Reaction-Diffusion Processes on Unstructured Meshes. *SIAM J. Sci. Comp.*, 31(3):1774–1797, 2009.

[12] R. Erban and S. J. Chapman. Stochastic modelling of reaction-diffusion processes: algorithms for bimolecular reactions. *Phys. Biol.*, 6(4):046001, August 2009.

[13] R. Erban, S. J. Chapman, and P. K. Maini. A practical guide to stochastic simulations of reaction-diffusion processes. `arXiv:0704.1908 [q-bio.SC]`, 2007.

[14] D. Fange, O. G. Berg, P. Sjöberg, and J. Elf. Stochastic reaction-diffusion kinetics in the microscopic limit. *PNAS*, 107(46):19820–19825, November 2010.

[15] L. Ferm, A. Hellander, and P. Lötstedt. An adaptive algorithm for simulation of stochastic reaction–diffusion processes. *J. Comp. Phys.*, 229(2):343–360, January 2010.

[16] C. W. Gardiner. *Handbook of Stochastic Methods: For*

Physics, Chemistry, and the Natural Sciences, volume 13 of *Springer Series in Synergetics*. Springer Verlag, New York, 2nd edition, 1996.

[17] C. W. Gardiner, K. J. McNeil, D. F. Walls, and I. S. Matheson. Correlations in stochastic models of chemical reactions. *J. Stat. Phys.*, 14:307, 1976.

[18] D. T. Gillespie. Exact stochastic simulation of coupled chemical-reactions. *J. Phys. Chem.*, 81(25):2340–2361, 1977.

[19] T. Hahn. Cuba–a library for multidimensional numerical integration. *Comp. Phys. Comm.*, 168(2):78 – 95, 2005.

[20] A. Hellander and P. Lötstedt. Incorporating active transport of cellular cargo in stochastic mesoscopic models of living cells. *Multiscale Modeling & Simulation*, 8(5):1691–1714, 2010.

[21] S. Hellander, A. Hellander, and L. Petzold. Reaction-diffusion master equation in the microscopic limit. *Phys. Rev. E*, 85(4):042901(1–5), April 2012.

[22] B. Hendriks, L. Opresko, H. Wiley, and D. Lauffenburger. Quantitative analysis of HER2-mediated effects on HER2 and epidermal growth factor receptor endocytosis. *J. Biol. Chem.*, (26):23343–23351, Jan 2003.

[23] S. A. Isaacson. Relationship between the reaction-diffusion master equation and particle tracking models. *J. Phys. A: Math. Theor.*, 41(6):065003 (15pp), 2008.

[24] S. A. Isaacson. The reaction-diffusion master equation as an asymptotic approximation of diffusion to a small target. *SIAM J. Appl. Math.*, 70(1):77–111, 2009.

[25] S. A. Isaacson and D. Isaacson. Reaction-diffusion master equation, diffusion-limited reactions, and singular potentials. *Phys. Rev. E*, 80(6):066106 (9pp), 2009.

[26] S. A. Isaacson, D. M. McQueen, and C. S. Peskin. The influence of volume exclusion by chromatin on the time required to find specific DNA binding sites by diffusion. *PNAS*, 108(9):3815–3820, March 2011.

[27] S. A. Isaacson and C. S. Peskin. Incorporating diffusion in complex geometries into stochastic chemical kinetics simulations. *SIAM J. Sci. Comput.*, 28(1):47–74, 2006.

[28] S. G. Johnson. Cubature integration library. Available at: `http://ab-initio.mit.edu/wiki/index.php/Cubature`.

[29] J. Keizer. Nonequilibrium statistical thermodynamics and the effect of diffusion on chemical reaction rates. *J. Phys. Chem.*, 86:5052–5067, 1982.

[30] F. Kühner, L. T. Costa, P. M. Bisch, S. Thalhammer, W. M. Heckl, and H. E. Gaub. LexA-DNA bond strength by single molecule force spectroscopy. *Biophys. J.*, 87:2683–2690, October 2004.

[31] L. Ma, J. Wagner, J. J. Rice, W. Hu, A. J. Levine, and G. A. Stolovitzky. A plausible model for the digital response of p53 to DNA damage. *Proc. Natl. Acad. Sci. USA*, 102(40):14266–71, Oct 2005.

[32] D. A. McQuarrie. Stochastic approach to chemical kinetics. *J. Appl. Prob.*, 4:413–478, 1967.

[33] J. Muñoz-García, Z. Neufeld, B. N. Kholodenko, and H. M. Sauro. Positional information generated by spatially distributed signaling cascades. *PLoS Comp. Biol.*, 5(3):e1000330, March 2009.

[34] S. Neves, P. Tsokas, A. Sarkar, E. Grace, P. Rangamani, S. Taubenfeld, C. Alberini, J. Schaff, R. Blitzer, I. Moraru, and R. Iyengar. Cell shape and negative links in regulatory motifs together control spatial information flow in signaling networks. *Cell*, 133(4):666–680, May 2008.

[35] J. Raser and E. O'Shea. Control of stochasticity in eukaryotic gene expression. *Science*, 304:1811–1814, Jan 2004.

[36] D.E. Shaw, R.O. Dror, J.K. Salmon, JP Grossman, K.M. Mackenzie, J.A. Bank, C. Young, M.M. Deneroff, B. Batson, and K.J. Bowers. Millisecond-scale molecular dynamics simulations on Anton. *Proceedings of the Conference on High Performance Computing Networking, Storage and Analysis*, page 39, 2009.

[37] M. V. Smoluchowski. Mathematical theory of the kinetics of the coagulation of colloidal solutions. *Z. Phys. Chem.*, 92:129–168, 1917.

[38] K. Takahashi, S. Tanase-Nicola, and P. R. ten Wolde. Spatio-temporal correlations can drastically change the response of a MAPK pathway. *PNAS*, 107(6):2473–2478, February 2010.

[39] E Teramoto and N Shigesada. Theory of bimolecular reaction processes in liquids. *Prog. Theor. Phys.*, 37(1):29–51, 1967.

[40] N. G. Van Kampen. *Stochastic Processes in Physics and Chemistry*. North-Holland, Amsterdam, 2001.

[41] M. Vigelius and B. Meyer. Multi-dimensional, mesoscopic Monte Carlo simulations of inhomogeneous reaction-drift-diffusion systems on graphics-processing units. *PloS one*, 7(4):e33384, April 2012.

[42] G. Von Dassow, E. Meir, E. M. Munro, and G. M. Odell. The segment polarity network is a robust developmental module. *Nature*, 406(6792):188–192, Jul 2000.

[43] H. Wang, C. S. Peskin, and T. C. Elston. A robust numerical algorithm for studying biomolecular transport processes. *J. Theor. Biol.*, 221:491–511, 2003.